Cluster Organization of Ion Channels Formed by the Antibiotic Syringomycin E in Bilayer Lipid Membranes

Yuri A. Kaulin,*# Ludmila V. Schagina,# Sergey M. Bezrukov,§¶ Valery V. Malev,# Alexander M. Feigin,* Jon Y. Takemoto,‖ John H. Teeter,* ** and Joseph G. Brand* **##

*Monell Chemical Senses Center, Philadelphia, Pennsylvania 19104-3308 USA; #Institute of Cytology of the Russian Academy of Sciences, St. Petersburg 194064, Russia; §National Institutes of Health, NICHD, Laboratory of Physical and Structural Biology, 5/405, Bethesda, Maryland 20892 USA; ¶St. Petersburg Nuclear Physics Institute of the Russian Academy of Sciences, Gatchina 188350, Russia; ‖Utah State University, Logan, Utah 84322-5305 USA; **University of Pennsylvania, Philadelphia, Pennsylvania 19104 USA; and ##Veterans Affairs Medical Center, Philadelphia, Pennsylvania 19104 USA

ABSTRACT The cyclic lipodepsipeptide, syringomycin E, when incorporated into planar lipid bilayer membranes, forms two types of channels (small and large) that are different in conductance by a factor of sixfold. To discriminate between a cluster organization-type channel structure and other possible different structures for the two channel types, their ionic selectivity and pore size were determined. Pore size was assessed using water-soluble polymers. Ion selectivity was found to be essentially the same for both the small and large channels. Their reversal (zero current) potentials with the sign corresponding to anionic selectivity did not differ by more than 3 mV at a twofold electrolyte gradient across the bilayer. Reduction in the single-channel conductance induced by poly(ethylene glycol)s of different molecular weights demonstrated that the aqueous pore sizes of the small and large channels did not differ by more than 2% and were close to 1 nm. Based on their virtually identical selectivity and size, we conclude that large syringomycin E channels are clusters of small ones exhibiting synchronous opening and closing.

INTRODUCTION

Multilevel conductance states have been found for many different types of ion channels (Geletyuk and Kazachenko, 1985; Fox, 1987; Meves and Nagy, 1989; Schreibmayer et al., 1989; Wateras et al., 1991; Larsen et al., 1996). However, for many of these channels, the nature of these multiple states remains obscure. It is possible that there exists a common mechanism for generating multilevel conductance states that may be independent of the particular structural features of a given channel. Use of artificial bilayer lipid membranes (BLMs) modified by an appropriate channel former offers a promising approach to the study of this phenomenon.

Syringomycin E (SRE) is a cyclic lipodepsipeptide (Fig. 1) produced by certain strains of the phytopathogenic bacterium *Pseudomonas syringae pv. syringae* (Sinden et al., 1971; Gross et al., 1977; Takemoto, 1992). SRE forms ion channels in lipid bilayers (Feigin et al., 1996). Ion channels formed by SRE in lipid membranes can serve as an appropriate model system for studying the mechanisms of the cluster organization and voltage-gated conductance of biological cell membrane ion channels.

Feigin et al. (1996) reported that SRE forms ion channels with weak anion selectivity in BLMs made from 1,2-dioleoyl-sn-glycero-3-phosphoserine in 0.1 M NaCl bathing solution. The kinetics of opening and closing, and the conductance of these channels, were strongly dependent on the applied voltage. When SRE was added to one side of the membrane, a positive potential on that side induced channel opening, resulting in an exponential increase in the membrane conductance. A shift of the voltage polarity from positive to negative induced channel closing, which resulted in a double-exponential decrease in the macroscopic conductance of the membrane over time. The conductance induced by SRE increased with the sixth power of SRE concentration, suggesting that at least six monomers are required for channel formation.

Here we report that in addition to the primary type of channel reported in the previous paper (Feigin et al., 1996), SRE also forms channels of about a sixfold lower conductance. These channels are referred to here simply as "large" and "small" channels, respectively.

The current work aims to discriminate between two possibilities: 1) whether the large channels are a result of aggregation of small channels, leading to their synchronous opening and closing, or 2) whether large and small channels correspond to two altogether different structures that are distinct in aqueous pore size and other transport parameters.

We first analyze the amplitude histograms and probability of appearance of SRE channels with different current amplitudes at different NaCl concentrations in the bathing solution. Second, we compare small and large channels, using the following approaches: 1) examining cation-anion selectivity of small versus large channels at different concentrations of NaCl; 2) studying the influence of the neutral polymers, poly(ethylene glycol)s, on the conductance of both the small and large channels.

The results of comparative analyses of the properties of the small and large channels demonstrate a high degree of

Received for publication 7 November 1997 and in final form 25 February 1998.

Address reprint requests to Dr. Joseph G. Brand, Monell Chemical Senses Center, 3500 Market St., Philadelphia, PA 19104-3308. Tel.: 215-898-5123; Fax: 215-898-2084; E-mail: brand@monell.org.

0006-3495/98/06/2918/08 $2.00

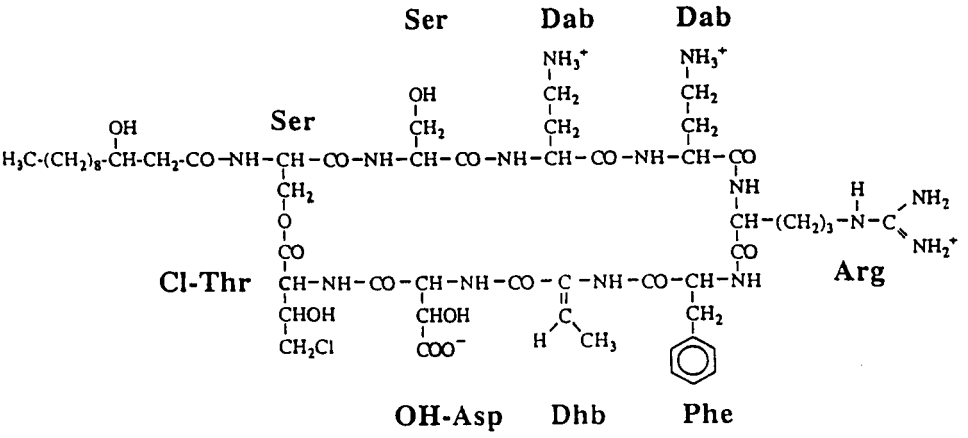

FIGURE 1 Syringomycin E (zwitterionic form). Arg, Arginine; OH-Asp, 3-hydroxyaspartic acid; Dab, 2,4-diaminobutyric acid; Dhb, dehydro-2-aminobutyric acid; Cl-Thr, 4-chlorothreonine; Ser, serine; Phe, phenylalanine.

similarity between the two channel types, suggesting that the large channels are clusters of the small ones. In addition, the pronounced sensitivity of the relative occurrence of large and small channels to the bulk salt concentration suggests that the channel clusters are stabilized by an interaction of the charged groups of SRE channels and those portions of the membrane lipids that are exposed to the membrane-bathing solution.

MATERIALS AND METHODS

Synthetic 1,2-dioleoyl-sn-glycero-3-phosphoserine (DOPS) and 1,2-dioleoyl-sn-glycero-3-phosphoethanolamine (DOPE) were purchased from Avanti Polar Lipids (Pelham, AL). All electrolytes were reagent grade (Sigma, St. Louis, MO). Water was doubly distilled and deionized. Salt solutions for bilayer experiments were in the range of 0.03–1.0 M NaCl buffered by 5 mM 3-(*N*-morpholino)propanesulfonic acid (MOPS) to pH 6.0. Syringomycin E was purified as described previously (Bidwai et al., 1987).

Virtually solvent-free membranes were prepared as described by Montall and Muller (1972). The membrane-forming solutions were DOPS and an equimolar mixture of DOPS and DOPE in hexane. Two symmetrical halves of a Teflon chamber with solution volumes of 1 cm^3 were divided by a 15-μm-thick Teflon partition containing a round aperture of ~100-μm diameter. Hexadecane in *n*-hexane (1:10, v/v) was used for aperture pretreatment. A pair of Ag-AgCl electrodes was used to maintain membrane potential and to detect current fluctuations. "Virtual ground" was maintained at the *trans* side of the bilayer. Hence positive voltages mean that the *cis*-side compartment is positive with respect to the *trans* side. Positive currents are therefore those of cations flowing from the *cis* to the *trans* side.

The cation-anion selectivity was determined by measuring the potential of zero current after formation of a twofold gradient of NaCl across the bilayer. The higher salt concentration was on the *cis* side.

Poly(ethylene glycol)s (PEGs) (Aldrich Chemical Co, Milwaukee, WI) were added to the 0.1M NaCl/MOPS buffer solution to achieve a 20% (w/w) concentration. PEG solution was added to both halves of the chamber after the membrane had been formed and modified by SRE. A potential of −150 mV was used throughout all experiments with PEG solutions.

Histograms were constructed from current amplitude changes at channel closings that were induced by negative voltage. For each current level the current amplitude histogram was fitted by a Gaussian distribution. The fit was carried out using Origin software (Microcal Software, Northampton, MA).

All experiments were performed at room temperature. A detailed description of methods used for membrane preparation and single-channel data analysis may be found elsewhere (Teeter et al., 1990; Bezrukov and Vodyanoy, 1993). Syringomycin E was added to the aqueous phase at one (*cis*) side of the bilayer from water stock solutions (1 mg/ml).

RESULTS AND DISCUSSION

SRE ion channels at different electrolyte concentrations

Several levels of current fluctuations are observed in membranes modified by SRE. These various levels are visible in sample records from different bath NaCl concentrations in Fig. 2. Note first that at least two different types of channels, large and small, are present. Second, the dwell time of the higher-conducting channels appears to be greater than that of the lower conducting ones. In addition, at low SRE concentration, <2 μg/ml, *cis* side only, the large channels are not observed (data not shown).

Fig. 3 illustrates the amplitude histograms of the SRE channel closings measured at a fixed transmembrane potential of −100 mV with different NaCl concentrations in the bathing solutions. A measure of the probability (P) (y axis) of the appearance of a particular channel type was calculated as N/N', where N is the number of current transitions corresponding to a particular conductance, and N' is the total number of transitions. P is directly proportional to the probability of finding a closing of a channel with a given level of current. From Fig. 3 it follows that

1. There are at least two peaks of current amplitude at each electrolyte concentration in the bathing solution.

2. At low NaCl concentrations (0.03 and 0.1 M) (Fig. 3, *A* and *B*) the ratio of the mean value of the second peak to that of the first peak is equal to ~6; however, at the high NaCl concentration (1.0 M) (Fig. 3 *C*), this ratio falls to ~2, and the number of channels with a unitary current amplitude of six times that of the small ones is extremely small. The respective P value for these large channels is equal to 0.004.

3. The relative number of large channels decreases with an increase in NaCl concentration, whereas the relative number of small channels increases (see also Fig. 2).

In general, the appearance of multiple levels of current fluctuations may be a result of the virtually simultaneous

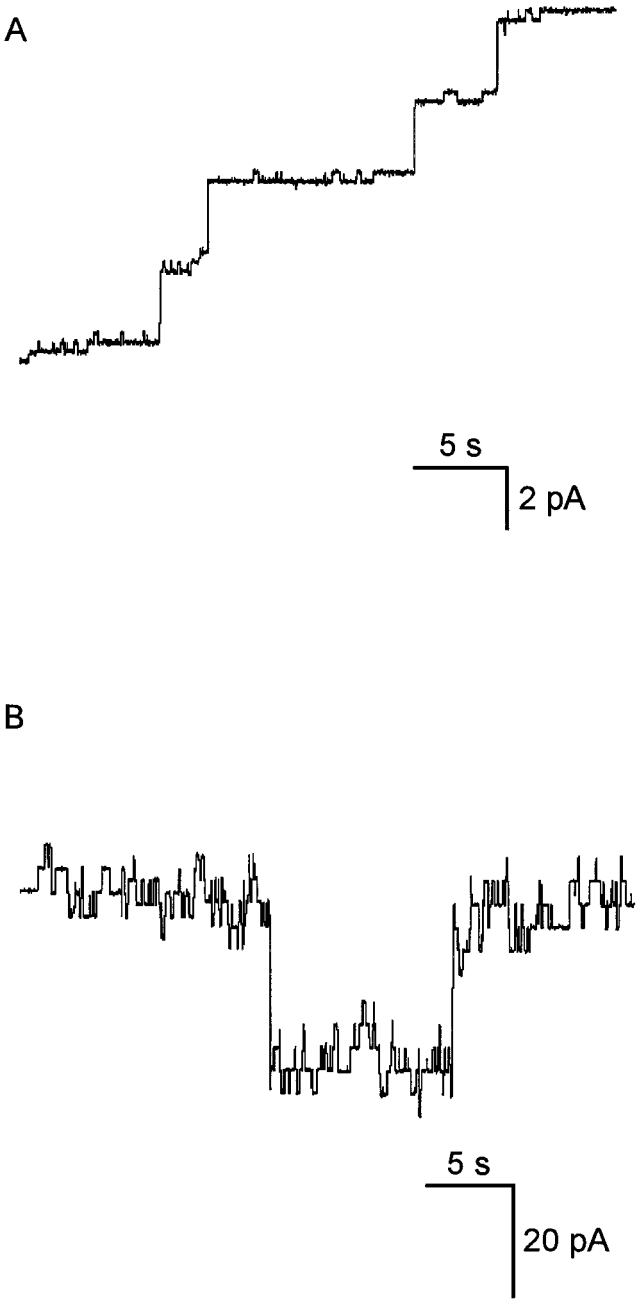

FIGURE 2 The records of transmembrane current fluctuations of bilayers made from DOPS/DOPE containing a few SRE channels at different salt concentration and negative applied voltage. (*A*) At 0.1 M NaCl, −100 mV. The concentration of SRE in the bathing solution (*cis* side only) was 5 μg/ml. (*B*) At 1 M NaCl, −100 mV. The concentration of SRE in the bathing solution (*cis* side only) was 7 μg/ml. Currents were filtered at 30 Hz.

random opening and closing of several independent channels that have equal conductance. Based on probability analysis, we have determined that (at 1 M NaCl) this assumption is, in fact, a likely explanation for the appearance of channels that have twice the unit current (9.4 pA) of the small channels. However, as the following analysis suggests, this assumption is not an appropriate explanation for the appearance of the large channels.

Routinely, statistical independence of ion channels is tested by comparing experimentally obtained histograms to a binomial distribution. An amplitude histogram is usually plotted as the number of counts in a narrow window around a particular current level as a function of the absolute value of this level. Such analysis determines the probability that one or several channels are open at the same time. If the channels are statistically independent, then the relative area under the nth peak should be close to the relative probability found from a corresponding binomial distribution for n channels being open simultaneously.

In the case presented here, the histograms in Fig. 3 have a different statistical meaning. Instead of describing the probability of finding n channels open simultaneously, the area under the nth peak represents the probability of n channels closing simultaneously: that is, closing within the time τ equal to the resolution time of our measurement. The corresponding experimental event is perceived as a closure of a larger channel. We wish to discriminate between a synchronous closing of several small channels organized into a cluster, and a random coincidence of several closings masked by the limited time resolution. If the channels are statistically independent, then their closings are also statistically independent events. The probability of finding exactly n events (channel closings) within a time τ at the average rate of events ν is given by (Rice, 1954)

$$P_n = \frac{(\nu\tau)^n}{n!}\exp(-\nu\tau) \tag{1}$$

Therefore, the relative probability of finding n independent channel closings, defined as the ratio to the probability of finding one channel closing, is

$$\frac{P_n}{P_1} = \frac{(\nu\tau)^{n-1}}{n!} \tag{2}$$

Given an average rate of channel closing of 0.5–2/s and a time resolution $\tau = 0.1$ s, we expect that the ratio of the probability of two channels closing simultaneously to the probability of one channel closing would be equal to 0.025–0.1. The ratio of the area under the second peak (S_2) to the area under the first peak (S_1) obtained from the results presented in the Fig. 3 *C* is equal to 0.12, which is close to our estimate for statistically independent channels. This analysis therefore suggests that the second peak in histogram Fig. 3 *C* corresponds to random simultaneous closings of two small channels.

For the large channels, which have a current that is six times higher, such an explanation is not viable. The experimental ratio of S_6/S_1 is equal to 6×10^{-4} (where S_6 is the area under the peak corresponding to the large channels), whereas the value P_6/P_1 calculated according to Eq. 2 is in the range of 4×10^{-7} to 4×10^{-10}. The difference between the experimental and theoretical values is more then three orders of magnitude, indicating that the large channels cannot be viewed as a random coincidence of the closing of six independent small channels.

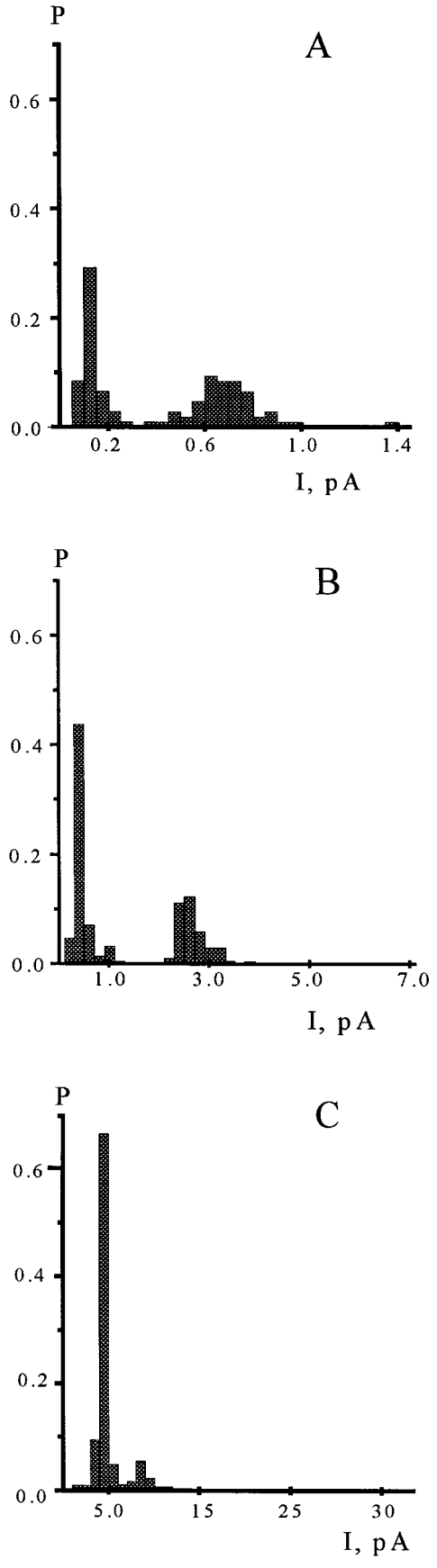

FIGURE 3 Amplitude histograms of current fluctuations measured at −100 mV transmembrane potential and different electrolyte concentrations in the bathing solutions. (*A*) 0.03 M NaCl; (*B*) 0.1 M NaCl; (*C*) 1 M NaCl. The *P* is calculated as N/N', where *N* is the number of current downward fluctuations corresponding to a particular conductance, and N' is the total number of fluctuations. (*A*) $N' = 104$; (*B*) $N' = 493$; (*C*) $N' = 1041$. The membranes were made from DOPS/DOPE.

For the more dilute bathing solutions (Fig. 3, *A* and *B*), the areas under peaks corresponding to the small and large channels are close to each other in value, and the ratio of the mean of the second distribution to the mean of the first distribution is equal to 6. The calculations according to Eq. 2 for these salt concentrations give a P_6/P_1 ratio several orders of magnitude less than the experimental ones. Again, these calculations suggest that the large channels are not the result of stochastic coincidences of opening or closing of six independent small channels. These results indicate that the large and small channels are either two sets of channels with altogether different structures or are a result of a synchronized opening and closing of six small channels organized into a single conducting unit.

Ion selectivity of large and small channels

If a large channel consists of six small ones organized into a conducting unit, it is reasonable to expect that cation-anion selectivities of the large and small channels should be practically the same. Earlier it was demonstrated that bilayers made from DOPS/DOPE and modified by SRE express an anion selectivity throughout a broad range of NaCl concentrations in the bathing solutions (0.01–1 M). In addition, the transfer numbers for Cl^- (t_{Cl^-}) decreased with increasing NaCl concentration (t_{a^-}) (0.83–0.70) (Kaulin et al., 1997; Schagina et al., 1998). Here we report that at each given concentration gradient, all conductance levels have the same ion selectivity (identical reversal potentials).

Fig. 4 shows records of the transmembrane current in the presence of a twofold electrolyte gradient across the bilayer (0.1 M NaCl, *cis* side; 0.05 M NaCl, *trans* side) at both −50 mV and −8 mV transmembrane potentials. The absence of any mean current or current fluctuations at −8 mV transmembrane potential indicates that all conductance levels have the same ion selectivity. Indeed, if the two types of channels had essentially different selectivity, we would have observed current jumps corresponding to opening or closing of small channels, or the closing of large channels. Such current jumps are never observed at this potential. In addition, the zero current potential remained the same during the experiment and did not depend on the value of the integral membrane conductance. These findings allow us to conclude that the large and small channels have the same anion-cation selectivity.

Data such as those shown in Fig. 4 allow a quantitative estimation of the difference between reversal potentials for small, E_S, and large, E_L, channels. Simple circuit considerations for a parallel arrangement of small channels with integral (total) conductance G_S, and for the large channels

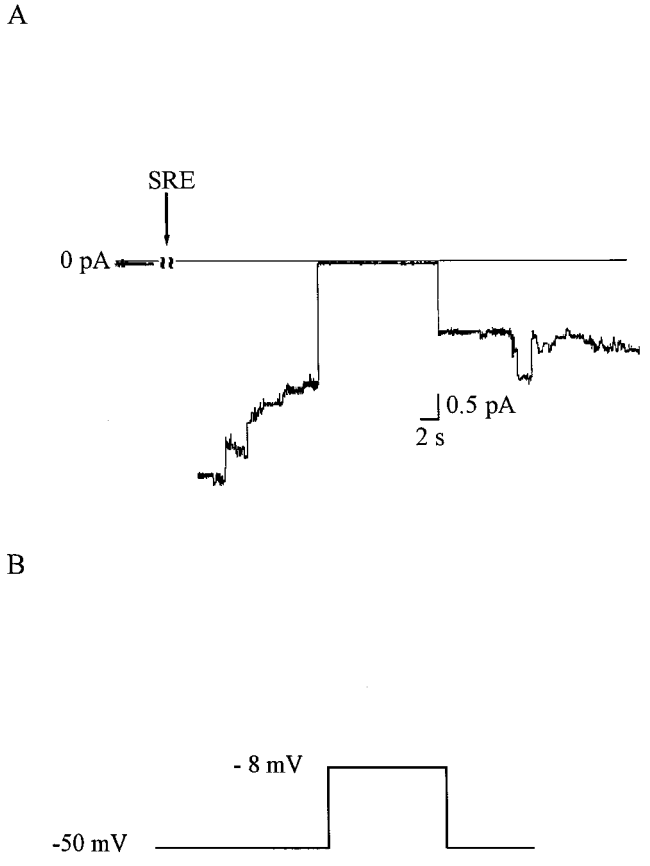

FIGURE 4 Representative experiment demonstrating the determination of ion selectivity of the membrane modified by SRE (5 μg/ml) in the presence of a twofold electrolyte gradient across the bilayer (0.1 M NaCl, *cis* side; 0.05 M NaCl, *trans* side). (*A*) Records of the transmembrane current at both −50 mV and −8 mV transmembrane voltages. (*B*) A drawing showing values of the applied potential.

with integral conductance G_L, show that the spontaneous opening or closing of a single large channel with conductance g_L would produce (in the measuring circuit) a current response δi that is related to the differences in reversal potential by the following expression:

$$\delta i = (E_L - E_S)\frac{g_L G_S}{G_L + G_S} \quad (3)$$

Then the upper estimate for the possible difference in reversal potentials for the large and small channels can be written as

$$|E_L - E_S| \le |(\delta i)_{min}|\frac{G_L + G_S}{g_L G_S} \quad (4)$$

where $|(\delta i)_{min}|$ is the amplitude of the smallest detectable long-lived stepwise deviation in the current from its zero value (the fragment of the record in Fig. 4 *A* corresponding to −8 mV). The ratio of integral conductances from the large and small channels in the experiment illustrated in Fig. 4 is close to 1. Using $|(\delta i)_{min}| \approx 3 \times 10^{-14}$ A and $g_L \approx 2 \times 10^{-11}$ S, we obtain $|E_S - E_L| < 3 \times 10^{-3}$ V; that is, reversal potentials for the small and large channels do not differ by more than 3 mV.

The observations of 1) identical anion selectivity of the small and large channels, as well as 2) integer multiple values of current fluctuations for these channels, may indicate that the large channels are clusters of the small ones.

Effect of water-soluble polymers on conductance of large and small channels

Additional evidence supporting the hypothesis of the cluster organization for the large channels has been derived from sizing of the channels by water-soluble polymers. This method allows one to size individual pores by using the change in the channel conductance that is induced by high concentrations of neutral polymers such as poly(ethylene glycol)s (Krasilnikov et al., 1992; Bezrukov and Vodyanoy, 1993; Korchev et al., 1995; Parsegian et al., 1995; Bezrukov et al., 1996; Desai and Rosenberg, 1997).

Fig. 5 displays samples of single-channel recordings in the absence and presence of PEG in the membrane bathing solution. Data of this figure show that the addition of PEG 200 reduced currents of both types of channels, whereas the addition of PEG 1500 had no effect on either of the conducting states. When a similar experiment was carried out with PEG 3400, an increase in the current fluctuations was observed. To compare the degree to which these nonelectrolytes permeated the channel pore, we measured the ratio of the channel conductance after PEG addition to the channel conductance before PEG addition. The dependence of this ratio on the PEG molecular weight is shown in Fig. 6.

Fig. 6 illustrates that for ethyleneglycol, PEG 200, and PEG 300, the effect on channel conductance is close to that seen with the bulk solution (*interrupted lines*). This observation indicates that these nonelectrolytes easily penetrate the SRE channels. Solutes PEG 400-1000 are also small enough to enter the channels, but large enough to display repulsive entropic interaction with the channel walls. As a result, the concentration of PEG inside the channel decreases and the conductance ratio grows.

The reason for the rise in channel conductance in solutions that contain PEGs with hydrodynamic radii that are either comparable to or larger than the channel radius itself is due to the fact that PEG binds water molecules, thereby increasing the activity of ions in the bathing solution (Bezrukov and Vodyanoy, 1993).

To analyze the above results quantitatively (Bezrukov et al., 1996), we assume that the polymer/weight-dependent reduction in the single-channel conductance, $\Delta g(w)$, is proportional to the polymer partition coefficient, $p(w)$,

$$\Delta g(w) \propto p(w) \quad (5)$$

and that the partition coefficient itself, defined as a ratio of the average monomer density inside the pore to that in the membrane bathing solution, can written in the form

$$p(w) = \exp(-(w/w_0)^{\alpha}) \quad (6)$$

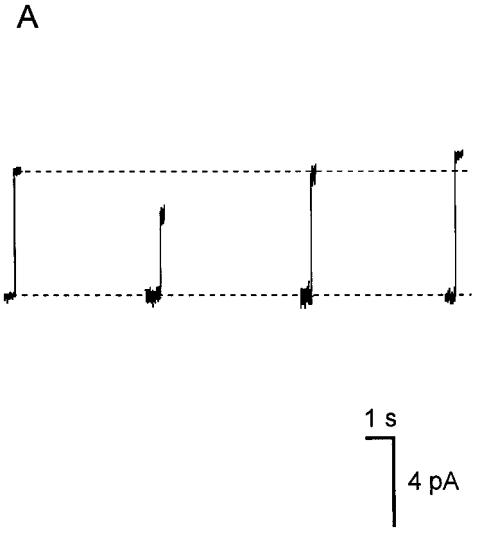

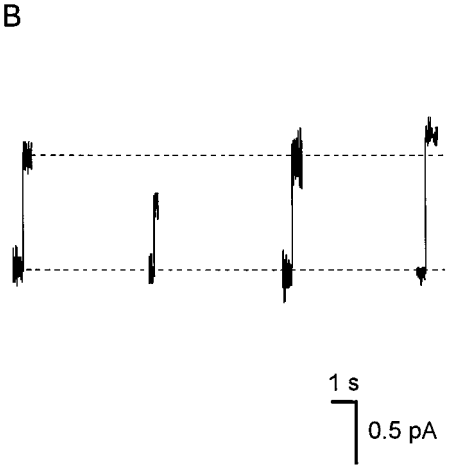

FIGURE 5 Effect of addition of different molecular weigh PEGs on the currents through the large (*A*) and small (*B*) SRE channels. From left to right: control (no PEG added), PEG 200, PEG 1500, PEG 3400.

Here w_0 is the ideal polymer molecular weight separating the penetrating and entropically excluded polymers. α is a parameter characterizing transition sharpness. Considering only entropic effects, the partition coefficient can be expressed through the free energy of polymer confinement in a pore, F_{conf}, as

$$p(w) = \exp(-F_{conf}/kT) \quad (7)$$

where k is the Boltzmann constant and T is the absolute temperature. A comparison of Eqs. 6 and 7 clarifies the meaning of w_0: the energy cost of transferring a polymer of this molecular weight from the bulk solution into the channel pore equals one kT.

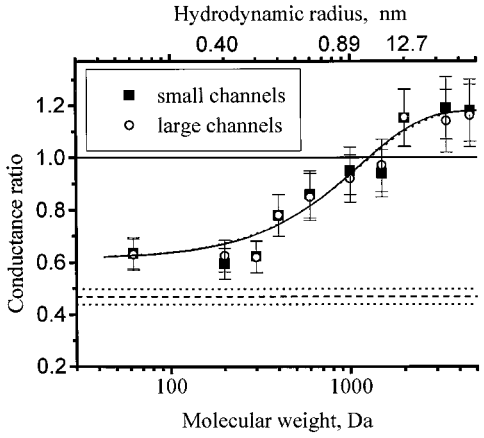

FIGURE 6 The dependence of a PEG-induced channel conductance change on the polymer molecular weight. Hydrodynamic radii of the polymers obtained from viscosity numbers or diffusion coefficients (Kuga, 1981) are presented on the top axis. The solid line corresponds to the unchanged channel conductance. The dashed line corresponds to the ratio of bulk conductivities of the solutions with and without polymers (*dotted lines* indicate the standard deviation). Solid and dotted curves through the data show the conductance ratio calculated from polymer partitioning that obeys Eq. 6 (see text).

Fitting Eqs. 5 and 6 to our data as described elsewhere (Bezrukov et al., 1996), we obtain $w_{0S} = 1.14 \times 10^3$ Da and $\alpha_S = 1.26$ for the small channels, and $w_{0L} = 1.16 \times 10^3$ Da and $\alpha_L = 1.22$ for the large channels. Corresponding plots are shown in Fig. 6 as solid and dotted curves. Because of the near identity of parameters obtained for the small and large channels, these two curves are indistinguishable.

The results presented here allow two general conclusions. First, the addition of solutes to the membrane bathing solution changes conductance of the large and small channels in the same way. Therefore the sizes of the two types of channels are indistinguishable from each other. Second, it can be tentatively concluded that radii of the large and small channels are approximately equal to 1 nm.

Comparison of the results presented here to data from the α-toxin channel (Bezrukov et al., 1996) shows that the ideal polymer molecular weight found in the present study is about 0.52 times smaller than that for α-toxin (1150 versus 2200). Taking into account that the linear size of the PEG random coil scales approximately as a square root of its weight, this observation suggests that the radius of the SRE channel pore is $\sqrt{0.52} \approx 0.72$ times smaller than the radius of the α-toxin pore. Available estimates for this radius (Krasilnikov et al., 1992; Olofsson et al., 1988) support the value of $\sim$1 nm for the SRE channel. Interestingly, partitioning of PEG into the α-toxin channel pore exhibits a much sharper transition between penetrating and excluded polymers, giving $\alpha = 3.1$. The reason for such a significant difference in sharpness of the conductance ratio/PEG weight curves for α-toxin and SRE (compare Bezrukov et al., 1996, and Fig. 6) is not clear at the moment. This difference may reflect deviations of the SRE channel pore geometry from a right cylinder, suggesting a conical shape for the SRE channel.

A pore radius of ~1 nm has been obtained from osmotic protection studies of erythrocytes modified by SRE (Hutchison et al., 1995). That study showed that the addition of PEG with radii greater than 1 nm fully protected erythrocytes from the lytic effect of SRE.

A similar value of channel radius for SRE has also been calculated from a recently developed theoretical approach (Schagina at al., 1998). This analysis allows estimation of a channel radius based on the experimental dependence of transfer numbers on the electrolyte concentration in the bathing solution.

The agreement in pore size from among such diverse approaches argues for the validity of our channel radius estimation. The fact that both types of channels have the same sieving size supports the hypothesis that the large channels are clusters of the small ones.

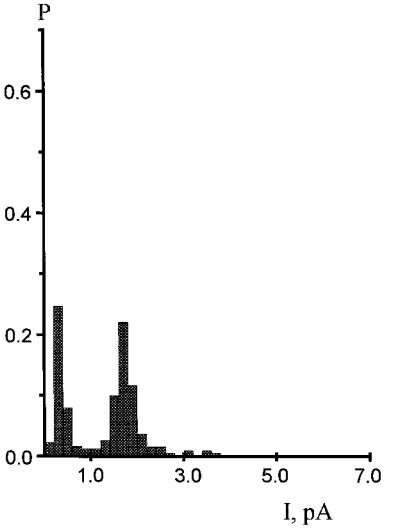

FIGURE 7 Amplitude histograms of current fluctuations measured in membranes from DOPS at −100 mV transmembrane potential and 0.1 M NaCl in the bathing solution. The *P* is calculated as described in the legend to Fig. 3, $N' = 299$.

On the mechanism of cluster stabilization: lipid effects

From Fig. 3 one can see that the probability of the appearance of large channels decreases with an increase in salt concentration in the bathing solution. The following consideration is useful in understanding this phenomenon. According to earlier data, it may be assumed that a channel is formed by six molecules of SRE (see Feigin et al., 1996) and, therefore, has 12 positive charges (Fig. 1). One can also assume that a certain number of lipid molecules are involved in forming the channel structure, because of electrostatic interactions of these charges with the negative charges on the lipid polar heads. If so, the interactions between different single channels via intermediate lipid molecules may stabilize SRE/lipid clusters containing several small channels. The synchronized opening and closing of several small channels organized in such a cluster provide the integer multiple conductance of the large channels that is seen in our experiments. Obviously, the probability of observing these clusters will diminish with increasing salt concentration. This must result from an inevitable decrease in the stability of the large channels due to a screening of the electric field of the SRE charges.

Such an explanation for the cluster stabilization is supported by additional observations obtained in experiments with bilayers of varying lipid composition. Fig. 7 shows that an increase in the negative charge of the membrane lipids promotes two effects. First, other conditions being equal, the probability of observing channel clustering increases when the lipid composition of the bilayer is changed from DOPS/DOPC mixture (Fig. 3 *B*) to pure DOPS (Fig. 7). Second, the conductance of the channel decreases in bilayers with increased negative charge.

Moreover, the charge on the channel (calculated from the above-referenced data on the dependence of the transfer number on the bath salt concentration; Schagina et al., 1998) is significantly smaller than that expected from the structural formula of the antibiotic. Schagina et al. (1998) calculated the charge on the channel wall as being equal to one electron charge. This value is an order of magnitude smaller than the charge value expected from purely structural considerations (i.e., 12 electron charges). This apparent discrepancy may be resolved by assuming that the charge on SRE molecules involved in the channel structure is compensated for, for the most part, by the charge of the lipid molecules adjacent to the channel. This observation supports the premise for the above-mentioned Coulombic interaction between neighboring small channels. Although the evidence reported and discussed above strongly supports the proposed hypothesis, further research is needed to develop a detailed cluster model.

CONCLUSIONS

1. Statistical analysis of currents through lipid bilayers induced by SRE shows that this antibiotic forms two types of channels with a sixfold difference in conductance.

2. The identical ion selectivities of the two types of channels, together with indistinguishable effects of solutes on their conductance, suggest that the large channels are clusters of the small ones.

3. Channel sizing by water-soluble polymers indicates that the radii of the channel aqueous pores in both small and large channels are approximately equal to 1 nm.

4. The decrease in the relative probability of observing large channels with an increase in bulk electrolyte concentration suggests that the clusters are stabilized by an interaction of charges of membrane lipids and SRE channels, oth at least partly exposed to the membrane-bathing solution.

This study was supported in part by the Russian Fund for Basic Research 97-04-49623 (to LVS); by a grant from the Department of Veterans Affairs

(to JGB); by a National Science Fouondation grant, IBN-9003398 (to JYT); by National Institutes of Health grants DC-00356 (to JGB) and DC-01838 (to JHT), and by the Utah Agricultural Experiment Station (project UTA 607).

REFERENCES

Bezrukov, S. M., and I. Vodyanoy. 1993. Probing alamethicin channels with water-soluble polymers. *Biophys. J.* 64:16–25.

Bezrukov, S. M., I. Vodyanoy, R. A. Brutyan, and J. J. Kasianowicz. 1996. Dynamics and free energy of polymers partitioning into a nanoscale pore. *Macromolecules.* 29:8517–8522.

Bidwai, A. P., L. Zhang, R. C. Bachmann, and J. Y. Takemoto. 1987. Mechanism of action of *Pseudomonas syringae* phytotoxin syringomycin. Stimulation of red beet plasma membrane ATPase activity. *Plant Physiol.* 83:39–43.

Desai, S. A., and R. L. Rosenberg. 1997. Pore size of the malaria parasite's nutrient channel. *Proc. Natl. Acad. Sci. USA.* 94:2045–2049.

Feigin, A. M., J. Y. Takemoto, R. Wangspa, J. H. Teeter, J. G. Brand. 1996. Properties of voltage-gated channels formed by syringomycin E in planar lipid bilayers. *J. Membr. Biol.* 149:41–47.

Fox, J. A. 1987. Ion channel subconductance states. *J. Membr. Biol.* 97:1–8.

Geletyuk, V. I., and V. N. Kazachenko. 1985. Single Cl^- channels in molluscan neurones: multiplicity of the conductance states. *J. Membr. Biol.* 86:9–15.

Gross, D. C., J. E. DeVay, and F. Stadman. 1977. Chemical properties of syringomycin and syringotoxin; toxigenic peptides produced by *Pseudomonas syringae. J. Appl. Bacteriol.* 43:446–453.

Hutchison, M. L., M. A. Tester, and D. C. Gross. 1995. Role of biosurfactant and ion channel-forming activities of syringomycin in transmembrane ion flux: a model for the mechanism of action in the plant-pathogen interaction. *Mol. Plant Microbe Interact.* 8:610–620.

Kaulin, Yu. A., V. V. Malev, L. V. Schagina, A. M. Feigin, M. P. Sidorova, J. Y. Takemoto, J. H. Teeter, and J. G. Brand. 1997. Estimation of lumen size of syringomycin E induced ion channels based on concentration dependence of transference numbers. *Biophys. J.* 72:A399.

Korchev, Y. E., C. L. Bashford, G. M. Alder, J. J. Kasianowich, and C. A. Pasternak. 1995. Low conductance states of a single ion channel are not "closed." *J. Membr. Biol.* 147:233–239.

Krasilnikov, O. V., R. Z. Sabirov, V. I. Ternovsky, P. G. Merzliak, and J. N. Muratkhodjaev. 1992. A simple method for determination of the pore radius of ion channels in planar lipid bilayer membranes. *FEMS Microbiol. Immunol.* 105:92–100.

Kuga, S. 1981. Pore size distribution analysis of gel substances by size exclusion chromatography. *J. Chromatogr.* 206:449–461.

Larsen, E. H., S. E. Gabriel, M. J. Stutts, J. Fullton, E. M. Price, and R. C. Boucher. 1996. Endogenous chloride channels of insect S*f*9 cell. Evidence for coordinate activity of small elementary channel units. *J. Gen. Physiol.* 107:695–714.

Meves, H., and K. Nagy. 1989. Multiple conductance states of the sodium channel and of other ion channels. *Biochim. Biophys. Acta.* 988:99–105.

Montall, M., and P. Muller. 1972. Formation of bimolecular membranes from lipid monolayers and study of their electrical properties. *Proc. Natl. Acad. Sci. USA.* 65:3561–3566.

Olofsson, A., U. Kaveus, M. Thelestam, and H. Herbert. 1988. The projection structure of alpha-toxin from *Staphylococcus aureus* in human platelet membranes as analyzed by electron microscopy and image processing. *J. Ultrastruct. Mol. Struct. Res.* 100:194–200.

Parsegian, V. A., S. M. Bezrukov, and I. Vodyanoy. 1995. Watching small molecules move: interrogating ionic channels using neutral solutes. *Biosci. Rep.* 15:503–513.

Rice, S. O. 1954. Mathematical analysis of random noise. *In* Selected Papers on Noise and Stochastic Processes. N. Wax, editor. Dover, New York. 133–294.

Schagina, L. V., Yu. A. Kaulin, A. M. Feigin, J. Y. Takemoto, J. G. Brand, and V. V. Malev. 1998. Properties of ion channels formed by the antibiotic syringomycin E in lipid bilayers: dependence on electrolyte concentration in the bathing solution. (in Russian) *Biol. Membr.* 15: 410–425.

Schreibmayer, W., H. A. Tritthart, and H. Schindler. 1989. The cardiac sodium channel shows a regular substate pattern indicating synchronized activity of several ion pathways instead of one. *Biochim. Biophys. Acta.* 986:172–186.

Sinden, S. L., J. E. DeVay, and P. A. Backman. 1971. Properties of syringomycin, a wide spectrum antibiotic and phytotoxin produced by *Pseudomonas syringae*, and its role in the bacterial canker disease of peach trees. *Physiol. Plant Pathol.* 1:199–213.

Takemoto, J. Y. 1992. Bacterial phytotoxin syringomycin and its interaction with host membranes. *In* Molecular Signals in Plant-Microbe Communications. D. P. S. Verma, editor. CRC Press, Boca Raton, FL. 247–260.

Teeter, J. H., J. G. Brand, T. Kumazawa. 1990. A stimulus-activated conductance in isolated taste epithelial membranes. *Biophys. J.* 58: 253–259.

Wateras, J., I. Bezprozvanny, and B. E. Ehrilich. 1991. Inositol 1,4,5-trisphosphate-gated channels in cerebellum: presence of multiple conductance states. *J. Neurosci.* 11:3239–3245.